Structural Effects in the Reductive Activation of [(indenyl)RhL_2] Complexes: the Reduction of the *anti* and *syn* Isomers of [$Cr(CO)_3$(indenyl)Rh(cod)]

Christian Amatore,*[a] Alberto Ceccon,[b] Saverio Santi,[b] and Jean Noël Verpeaux[a]

Dedicated to Professor René Poilblanc on the occasion of his retirement from the Université Paul Sabatier, Toulouse, France

Abstract: The electrochemical reduction of *anti*- and *syn*-[$Cr(CO)_3$(indenyl)Rh(cod)] complexes (cod = cyclooctadiene) has been investigated, to evaluate, in each stereochemical situation, the effects of the contemporary presence of two metals coordinated to the indenyl ligand. In contrast to the reduction of monometallic [(indenyl)Rh(cod)], which gives rise to two well separated monoelectronic waves, the reduction of both bimetallic complexes occurs at more positive potentials in a single bielectronic and chemically reversible wave. These results indicate that an $EC_{rev}E$ mechanism is active, in which the chemical step following the first electron transfer is the reversible structural rearrangement of the 35-electron radical anion, which allows the second electron transfer to occur at a more positive potential than the first one. This structural rearrangement is more marked when the two metals are *syn*, which suggests the presence of an interaction between the two metals in this configuration. Side reactions correspond to the dissociation of the mono- and dianions; yet the dianions are surprisingly less frangible than the monoanions.

Keywords: arene complexes · carbonyl complexes · chromium · electron transfer · rhodium

Introduction

The paramagnetic species generated by addition or uptake of one electron from a stable compound are very often recognised as the key intermediates in many catalytic cycles, even if the initial electron transfer (ET) activation process is not clearly identified.[1] In a recent paper,[2] we reported a study on the electrochemical reduction of the [(indenyl)Rh(cod)] complex and the reactivity of the corresponding mono- and dianion towards free cycloctadiene. Those results established the ET-tunable change of hapticity of the indenyl ligand, which we related to the formation of 17- and 19-electron metal-centred intermediates.

In most cases, the ET induces a profound chemical reorganisation of the structure, which makes the complex prone to react chemically. Yet, the drawback is often that the intermediate formed after the ET is so activated (note that the transfer of one electron over one volt amounts to the injection of 23 Kcal mol^{-1}) that several reaction pathways are generally opened, which leads to a poor selectivity. In the case of bimetallic complexes, the situation can be depicted as two coordination shells with possible interactive effects between the two metal centres. Since electronically cooperative bimetallic centres are more prone to stabilise one extra electron (or hole), the corresponding radical ions are often fairly stable and several studies have aimed to characterise the coupling of the unpaired electron with centres in terms of "electronic communicability".[3] However, bimetallic or polymetallic centres (clusters) are also catalysts and are frequently more efficient and more selective than the corresponding monometallic analogues, which fully justifies the importance of studying their ET activation. In this respect, it seems worthwhile to be able to control the energy release to the metal centre M_{cat} of interest, namely to that where the sought catalytic reaction should occur (Scheme 1). A solution to the problem consists in designing structures in which one metal centre, M_{ant}, plays the role of an electron (or hole) antenna, which upon ET activation is able to shuttle selectively part of the energy gained to a second centre through chemical modification of their common coordination sphere.

The concept of "topo-chemical communicability" can be invoked for those compounds where the activation of one metal centre by an electron transfer or the addition of a ligand would result in a structural modification responsible for the chemical (not the redox) activation of the second centre. This tandem activation, which differs from the "electronic com-

[a] Dr. C. Amatore, Dr. J.-N. Verpeaux
Département de Chimie de l'Ecole Normale Supérieure
UMR 8640 PASTEUR
24 rue Lhomond, F-75231 Paris Cedex 05 (France)
Fax: (+33) 1-4432-3863
E-mail: amatore@junie.ens.fr

[b] Dr. A. Ceccon, Dr. S. Santi
Università degli Studi di Padova, Dipartimento di Chimica
Fisica Via Loredan 2, I-35131 Padova (Italy)
E-mail: s.santi@chfi.unipd.it

  0947-6539/99/0511-3357 $ 17.50+.50/0

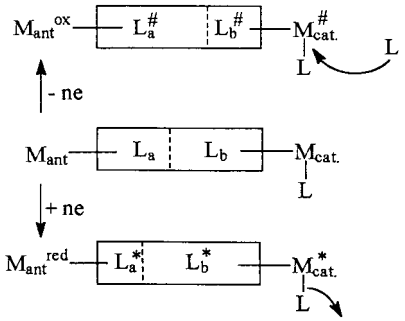

Scheme 1.

municability" in which the tandem activation occurs by means of electronic delocalisation or internal ET, may appear somewhat idealistic. However, it should be kept in mind that it actually governs a lot of fundamental biological processes, which require a separation of charges.[4]

Within this framework, it appears that the presence of a bridging ligand is required. In this respect, indenyl is a good candidate since its hapticity (from 1 to 6) may be governed by the oxidation state, electronic properties and the total number of ligands of the coordinated metal centre.[5] Also of great interest when two metals are coordinated to the same indenyl ligand is that the control of the oxidation state of one of the metal centres M_{ant} (namely antenna) should lead to a modification of its electronic demand to the shared ligand. This in turn forces a change of hapticity at the second (namely catalytic) metal centre M_{cat} that will eventually control further modifications of this latter coordination shell (Scheme 1). The redox changes on the antenna should allow a fine tuning of the chemical reactivity of the true catalytic centre by means of a structural modification of its ligand sphere. In this respect, it is worth emphasising that this concept is quite different from that of "electronic communicability" between redox centres, which occurs by means of electronic delocalisation or internal electron exchange.[3]

The above concept requires the confluence of two factors.

1) One must be able to induce changes in the topology of the indenyl ligand by redox changes on the first centre.
2) Structural modification of the indenyl ligand should result in a chemical activation of the second metallic centre.

$[(In)RhL_2]$(In = indenyl) complexes have proven to be very efficient catalysts for hydroacylation of olefins, cyclotrimerisation of alkynes or even CH bond activation of alkanes.[6] The "indenyl effect" is quite strong in this series since it was shown that the rate of exchange of ligand L becomes 10^8 times faster when the cyclopentadienyl ligand in $CpRhL_2$ is replaced by the indenyl. Three more orders of magnitude are gained when a tricarbonylchromium group is coordinated to the six-membered ring.[6, 7] This establishes the experimental validity of the second requirement above, which shows that the most critical point of the above somewhat idealistic concept relies in fact on the validity of the first requisite. We wish to present evidence that this is actually the case by examining the effect of the ET activation in the bimetallic *anti* and *syn* isomers of $[Cr(CO)_3$(indenyl)Rh(cod)] (cod = cyclooctadiene). $[Cr(CO)_3$(indenyl)Rh(cod)] was denoted by [CTC(In)Rh(cod)] in the following (CTC = chromium tricarbonyl).

Results

Electrochemical reduction of *anti*- and *syn*-$[Cr(CO)_3$(indenyl)Rh(cod)]: The reduction of both isomers, the *anti* represented by **1** and the *syn* represented by **2**, led to analogous cyclic voltammograms, as illustrated in Figure 1a (solid line for **1**, dashed line for **2**), for a 2.2 mM solution of complex in THF/0.15 M $nBu_4N \cdot BF_4$ at 0.5 V s^{-1}. In either case, the voltammogram exhibits one apparently chemically reversible reduction wave, with a rather broad peak-to-peak

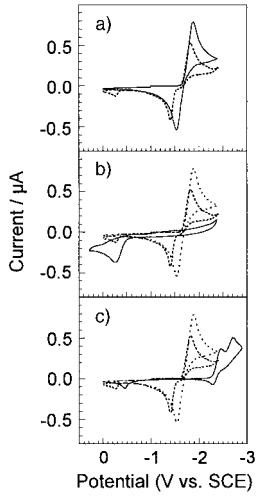

Figure 1. Voltammetric reduction of *anti*- and *syn*-$[Cr(CO)_3$(indenyl)Rh(cod)] (2.2 mM) in THF (0.3 M) nBu_4BF_4 at a gold disk electrode (0.5 mm diameter); $\nu = 0.5$ V s^{-1}, 20 °C. a) solid line for the *anti* isomer, dashed line for the *syn* isomer; b) after electrolysis at −2.1 V vs. SCE (solid line) superimposed to the previous voltammograms (a) shown now in dotted line; c) reduction of [(indenyl)Rh(cod)] (solid line) superimposed to the voltammograms shown in (a) in dotted line.

separation: $E^p = -1.89$ V vs. SCE (saturated calomel electrode), $\Delta E^p = E^p_{ox} - E^p_{red} = 360$ mV for **1** and $E^p = -1.82$ V vs. SCE, $\Delta E^p = E^p_{ox} - E^p_{red} = 440$ mV for **2**.[8] The peak current associated with the reduction wave is not proportional to $\nu^{1/2}$ as would be expected for a simple reversible process;[9] the current function $i^p\nu^{-1/2}$ increases with decreasing potential scan rate. Figure 2 shows the variation of this current function—normalised to its value at high scan rate—with the potential scan rate.

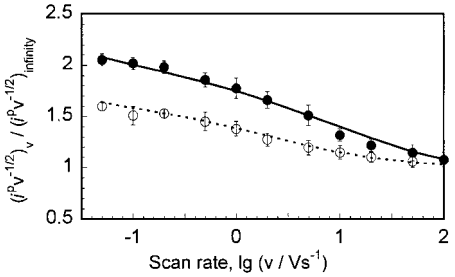

Figure 2. Variations of the current function normalised to its value at infinite scan rate ($\nu \geq 100$ V s^{-1}) of the reduction wave of *anti*- (solid line) and *syn*- (dashed line) $[Cr(CO)_3$(indenyl)Rh(cod)] (2.2 mM) in THF (0.3 M) nBu_4NBF_4 at a gold disk electrode (0.5 and 0.125 mm diameter according to the scan rate), 20 °C. Symbols: experimental data; solid or dotted lines: theoretical variations based on the results of simulation; for the kinetic parameters used, see the Experimental Section.

0947-6539/99/0511-3358 $ 17.50+.50/0 *Chem. Eur. J.* **1999**, *5*, No. 11

For the *anti* isomer, this normalised current function increases from one, at high scan rate, to approximately two at low scan rates; determination of the absolute electron stoichiometry[10] at sufficiently low scan rate ($n_{app} = 2.0 \pm 0.4$ at $\nu \leq 0.1$ V s^{-1}) confirmed that, within this time scale, the reduction wave is bielectronic. The *syn* isomer behaves similarly, except that the current function remains smaller than two (Figure 2 dashed line), in agreement with the measured value of $n_{app} = 1.73 \pm 0.35$ at $\nu \leq 0.1$ V s^{-1}. It must be pointed out that the overall reduction wave of either isomer remains reversible chemically within the range of the scan rate investigated.

In contrast, preparative scale electrolytic reduction, carried out on one isomer or the other, requires only one Faraday at this longer time scale and yields η^6-indenyl tricarbonylchromate $[(CO)_3Cr(In)]^-$, (denoted as $[CTC(In)]^-$, quantitatively. The final voltammogram (identical for either isomer), obtained after consumption of one electron *per* mole (Figure 1b solid line), displays only one oxidation wave ($E^p = -0.25$ V at 0.5 V s^{-1}) corresponding to $CTC(In)^-$. This could be checked with an authentic sample generated by in situ deprotonation of $[Cr(CO)_3(indene)]$.

In fact, this oxidation wave is already present in the cyclic voltammograms obtained from complex **2** for the whole range of scan rates (Figures 1 and 3d–f). The wave indicates that the formation of $CTC(In)^-$ from the reduced *syn* isomer takes place, at least to some extent, on the time scale of cyclic voltammetry. This supports qualitatively the difference in voltametric electron stoichiometry noted above, since this wave features a one-electron pathway. A different situation is encountered with the *anti* isomer **1**, for which the cyclic voltammogram displays a different oxidation wave ($E^p = -0.35$ V at 5 V s^{-1}). The size of the wave increases with the potential scan rate and the wave is practically absent at $\nu = 0.5$ V s^{-1} but clearly visible at 5 V s^{-1} and above (Figure 3a–c). Finally, two other oxidation waves are also present on the reverse scan following the reduction of the *syn* isomer **2** (Figures 3d–e) but these do not occur for **1**. The waves are located at -1.6 (shoulder) and -0.8 V and they originate (see below) from the rhodium fragment Rh(cod).[11]

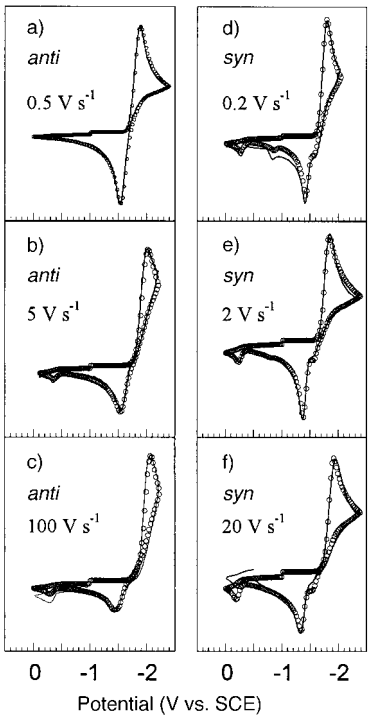

Figure 3. Experimental (solid line) and simulated (open circles) voltammetric reduction of *anti*- and *syn*-$[Cr(CO)_3(indenyl)Rh(cod)]$ (2.2 mM) in THF (0.3 M) nBu_4NBF_4 at a gold disk electrode (0.5 mm diameter) 20 °C; a) isomer *anti* at $\nu = 0.5$ V s^{-1}, b) isomer *anti* at $\nu = 5$ V s^{-1}, c) isomer *anti* at $\nu = 100$ V s^{-1}, d) isomer *syn* at $\nu = 0.2$ V s^{-1}, e) isomer *syn* at $\nu = 2$ V s^{-1}, f) isomer *syn* at $\nu = 20$ V s^{-1}.

Discussion

Qualitative analysis of the cyclic voltammetry behaviour

The bielectronic reversible wave: *an $EC_{rev}E$ mechanism controlled by the rates of the heterogeneous electron transfers*: The reduction of *syn* and *anti* isomers of $[Cr(CO)_3(indenyl)Rh(cod)]$ appears as a chemically reversible monoelectronic process at high potential scan rate ($\nu > 20$ V s^{-1}); upon decreasing the scan rate, the reduction tends to and finally becomes (isomer **1**) a bielectronic process, which is still a chemically reversible process at a lower scan rate. This is characteristic of an $EC_{rev}E$ mechanism in which the radical anion formed after the first electron transfer undergoes a reversible chemical transformation, which leads to a product reducible at the potential of the first electron transfer. At a sufficiently high scan rate, the forward reaction of the chemical step is kinetically "frozen" and the scheme is restricted to the first reversible electron transfer. When the time scale increases, the reducible product formed by the chemical step is significantly formed, which leads to the progressive increase of the current function from 1 to 2. The fact that the two electron reduction waves never appear chemically irreversible indicates that both the forward and backward reactions of the chemical step become operative almost in the same time scale, which means that the forward rate constant k_{1f} cannot be significantly different from the backward rate constant k_{1b}. In other words, in both cases the interposed chemical step is almost isoenthalpic ($\Delta G^0 \approx 0$).

The reversible chemical step involved in this $EC_{rev}E$ process cannot be the cleavage of the rhodium–indenyl bond, as established in the case of the monometallic analogue;[2] indeed, in the latter case, the rhodium fragment Rh(cod) is necessarily reduced at the very negative potential, at which the reduction of the parent monometallic complex ($E^0 = -2.35$ V) takes place. However, this fragment cannot be reduced at the less negative reduction potentials for the bimetallic species **1** or **2**. Therefore, a two-electron reversible reduction could not be observed. This crucial point was demonstrated by an independent study of the electrochemical behaviour of $[Rh(cod)(THF)_2]^+$ as well as $[\{Rh(cod)Cl\}_2]$, which allowed us to determine the reduction potential of the [Rh(cod)] radical at $E^p = -2.15$ V.[11]

For this reason, and because of the presence of only one reduction wave for the bimetallic complex (whereas two, one for the formation of the monoanion and one for the dianion,

were visible for the monometallic analogue[2]), a structural rearrangement of the monoanion from a form A^- to a readily reducible form B^- precursor of the dianion B^{2-} has been considered [Eq. (1) – (3)] as the reversible reaction C_{rev}, which takes place on the time scale of a few milliseconds.

Main reversible reduction wave: $EC_{rev}E$ *system.*

$$[CTC(In)Rh(cod)] + e \rightleftharpoons [CTC(In)Rh(cod)]_A^- \quad E_1^0,\ k_1^0,\ \alpha_1 \quad (1)$$

$$[CTC(In)Rh(cod)]_A^- \rightleftharpoons [CTC(In)Rh(cod)]_B^- \quad k_{1f},\ k_{1b},\ K_1 = k_{1f}/k_{1b} \quad (2)$$

$$[CTC(In)Rh(cod)]_B^- + e \rightleftharpoons [CTC(In)Rh(cod)]_B^{2-} \quad E_2^0,\ k_2^0,\ \alpha_2 \quad (3)$$

Cleavage of the monoanion [Eq. (4) – (5)].

$$[CTC(In)Rh(cod)]_{A/B}^- \rightleftharpoons [CTC(In)Rh(cod)]_C^- \quad k_{2f},\ k_{2b},\ K_2 = k_{2f}/k_{2b} \quad (4)$$

$$[CTC(In)Rh(cod)]_C^- \longrightarrow CTC(In)^- + Rh(cod) \quad k_3 \quad (5)$$

In those time scales where the equilibrium is labile, the apparent standard potential of the bielectronic reduction wave normally depends on both E_1^0 and E_2^0, as well as K_1.[12] [Eq. (6)].

$$E_{app}^0 = (E_1^0 + E_2^0)/2 + (RT/2F)\ln K_1 \quad (6)$$

This square scheme situation, an example of which is the well-known hydroquinone/quinone system, leads to the reversible bielectronic wave being situated in between the two reversible monoelectronic waves, which correspond to the reduction of A (redox couple A/A^-) in one case and the oxidation of B^{2-} (redox couple B^-/B^{2-}) in the other case. Both processes take place more easily than expected from their thermodynamics, as a result of the kinetics of the labile equilibrium.[9] However, in the system described here, the situation looks slightly different because it involves slow and eventually rate-determining heterogeneous electron transfers. These are responsible for the broad peak-to-peak separation observed even at low potential scan rate ($\Delta E^p = E_{ox}^p - E_{red}^p =$ 360 mV for **1** and 440 mV for **2** at 0.5 $V s^{-1}$) and for the width of the waves measured by $(E^{p/2} - E^p)$ (Figure 4). Under such conditions, the position of the reduction wave is mostly determined by the thermodynamic (E_1^0) and kinetic (k_1^0, α_1) parameters of the heterogeneous electron transfer from the electrode to the neutral species. The position of the oxidation wave is determined by the related parameters of the electron transfer from the dianion to the electrode.[9] The peak current (Figure 2) is far less affected by this phenomenon and remains governed by the extent of the rearrangement, which leads to the second electron transfer.

The cleavage process, a two-step pathway from the monoanion: Preparative scale electrolysis showed that the final reduction product of either isomer is the indenyl tricarbonylchromate $[CTC(In)]^-$, which was obtained in a quantitative yield after consumption of one Faraday; the neutral rhodium fragment or its evolution products were not characterised.

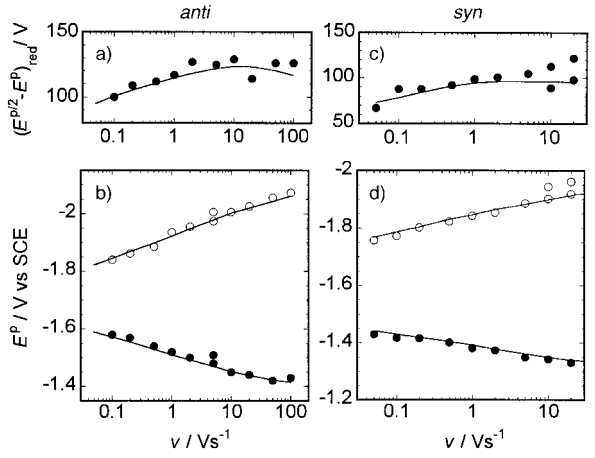

Figure 4. Experimental (solid line) and simulated (circles) data concerning the main reversible reduction wave of *anti*- and *syn*-[Cr(CO)$_3$(indenyl)Rh(cod)] (2.2 mM) in THF (0.3 M) nBu_4NBF_4 at a gold disk electrode (0.5 mm diameter) 20 °C; a) and c) variation of the half peak width $(E^{p/2} - E^p)_{red}$ for the reduction wave as a function of log(ν): a) *anti*, c) *syn*; b) and d) variation of the peak potentials E_{red}^p (open circles) and E_{ox}^p (full circles) vs. log(ν): b) *anti* and d) *syn*.

In the case of the *syn* isomer, this cleavage takes place partially on the time scale of cyclic voltammetry and the oxidation wave of $[CTC(In)]^-$ is visible in the whole range of potential scan rates at approximately -0.2 V vs. SCE (Figure 3d – e). This is crucial since it indicates that on the shorter time scales, when the reduction is monoelectronic (Figure 2), that is when the dianion is not formed, the formation of $[CTC(In)]^-$ already occurs; it establishes that the cleavage works on the monoanion. At lower scan rates, when the A^- to B^- rearrangement is fully operative and the dianion has formed for a significant time, the wave at -0.2 V is less developed. This is a further confirmation that the monoanion is the main source of $[CTC(In)]^-$ as it is less stable than the dianion with respect to its cleavage. In the case of the *anti* isomer, the cleavage does not take place on the time scale of cyclic voltammetry. However, the oxidation wave at around -0.35 V proves the formation of an intermediate complex (represented by C^-); the fact that this oxidation wave is very visible at scan rates as high as 100 $V s^{-1}$ (Figure 3c) indicates that this intermediate is formed from a monoanion. That it disappears at low scan rates and is totally absent at 0.5 $V s^{-1}$ proves that the process yielding the C^- intermediate is fully reversible.

Since the *syn* and *anti* isomers exhibit similar behaviour with regard to the main reversible reduction peak and their fate in preparative scale electrolysis as well, we are forced to consider that the cleavage processes are analogous despite the difference observed in cyclic voltammetry. Indeed both voltammetric patterns can be explained by a common two-step pathway, which consists of a reversible reaction leading to C^- [Eq. (4)], followed by an irreversible cleavage of C^- leading to $[CTC(In)]^-$ and the rhodium fragment [Eq. (5)].[13] However, the rate constant k_3^{anti} is too slow for the cleavage to take place on the time scale of slow cyclic voltammetry and the scheme is limited to reactions 1 to 4, and the oxidation of C^- at -0.35 V. Conversely, k_3^{syn} is high enough to drive part of the reversible dynamic system to the final

0947-6539/99/0511-3360 $ 17.50+.50/0 *Chem. Eur. J.* **1999**, *5*, No. 11

fragmentation. This partial irreversible loss of some monoanionic bimetallic species on the time scale of voltammetry accounts for the lower limit of the normalised current function for the *syn* isomer, since the corresponding pathway accounts for one electron in the overall stoichiometry.

Rates and mechanism of the reduction process using digital simulation: The mechanism shown in Equations (1)–(5) and proposed on the basis of cyclic voltammetry at different scan rates and preparative scale electrolyses needs to be ascertained on quantitative grounds. This requires the use of digital simulation because of the complexity of the scheme. The rate constants are far too numerous to allow a significant blind search for a fitting set of values. This operation must be performed step by step and the approach sticks to the qualitative analysis described above: the characteristics of the main reversible reduction wave were determined first and the parameters related to the chemical follow-up reactions were then introduced progressively in a second stage.

Since the intrinsic slowness of the two heterogeneous electron transfer steps [Eq. (1) and (3)] governs primarily both the position E^p and shape (half width) of the reduction and subsequent oxidation waves, the corresponding transfer coefficients α had to be determined first. Voltammograms at high potential scan rate, that is when the reduction process is mainly restricted to Equation (1) without the interference of any homogeneous kinetics (plateau value in Figure 4a and c), were used to measure α_1 associated with the cathodic wave. The half peak width value ($E_{p/2} - E_p = 47.7/\alpha n_\alpha$) gave $\alpha_1^{anti} = 0.39$ and $\alpha_1^{syn} = 0.5$, whereas another determination of the same coefficients based on the peak potential shift with the potential scan rate ($\Delta E_p = 29.6/\alpha n_\alpha$ per decade of ν) led to $\alpha_1^{anti} = 0.43$ and $\alpha_1^{syn} = 0.6$.[9] The average values $\alpha_1^{anti} = 0.41$ and $\alpha_1^{syn} = 0.55$ were then used in the digital simulations. The thermodynamic (E_1^0) and heterogeneous rate constants of the first electron transfer ($k_1^{0anti} = 2.0 \times 10^{-3}$ and $k_1^{0syn} = 3.5 \times 10^{-2}$ cm s^{-1}) were then adjusted from the peak potential position of the reduction wave in the same range of scan rates.

The parameters α_2 and k_2^0 relating to the second electron transfer ($B^- \longrightarrow B^{2-}$) can be extracted in a similar way from the reverse oxidation wave, under conditions where this wave actually corresponds to the oxidation of the dianion B^{2-} (the initial electron transfer being again determining) and not to the oxidation of A^-. The voltammograms at low potential scan rate (0.1 to 5 V s^{-1}) were then used. The shift of the peak potential with the scan rate ($\Delta E_p = 29.6/(1-\alpha)n_\alpha$ per decade of ν) meant that $(1-\alpha_2^{anti}) = 0.5$ and $(1-\alpha_2^{syn}) = 0.8$. The thermodynamic (E_2^0) and heterogeneous rate constants of the second electron transfer ($k_2^{0anti} = 4.0 \times 10^{-3}$ and $k_2^{0syn} = 4.5 \times 10^{-2}$ cm s^{-1}) were also adjusted from the peak potential position.

Whereas the position of the reduction (and backward oxidation) wave is set by the thermodynamics and kinetics of the initial heterogeneous electron transfers, the current is essentially related to the kinetics of the homogeneous chemical reactions: the shift from one to two electrons reflects:

1) The possibility to settle the dynamic equilibrium between A^- and B^- (rate constants k_{1f} and k_{1b}), which controls the second electron transfer.
2) The competition between this bielectronic reduction to B^{2-} and the monoelectronic pathway leading first to C^- and eventually to the cleavage (rate constants k_2 and k_3).

The parameters k_{1f} and k_{1b} have been adjusted to reproduce the experimental cathodic peak current function of the reduction wave (Figure 2); more precisely, k_{1f} was optimised from the peak current of the cathodic wave in the range of higher scan rates ($\nu \geq 5$ V s^{-1}) and then k_{1b} was extracted from the same peak current in the range of lower scan rates. The best fittings were obtained for $k_{1f}^{anti} = 150$ s^{-1}, $k_{1b}^{anti} = 150$ s^{-1}, $k_{1f}^{syn} = 100$ s^{-1} and $k_{1b}^{syn} = 600$ s^{-1}.

In the case of isomer **1**, the competition parameter $k_{2f}^{anti}/k_{1f}^{anti}$ was then introduced and optimised from the values of the reduction and oxidation peak currents measured in the whole range of scan rates. Finally the rate constant k_{2b}^{anti} has been adjusted to simulate the dependence with the scan rate of the size of the oxidation wave of C^- visible at -0.35 V [Eq. (7)].

$$[CTC(In)Rh(cod)]_{C^-} - e \rightleftharpoons [CTC(In)Rh(cod)]_C \longrightarrow .. \quad E_3^0,\ k_3^{0anti},\ \alpha_3^{anti} \qquad (7)$$

It was not possible to distinguish which of the two forms of the monoanion (A^- or B^-) was actually responsible for the follow-up reaction [Eq. (4)], since the results of digital simulation ($k_{2f}^{anti} = 100$ s^{-1}, $k_{2b}^{anti} = 100$ s^{-1}) were practically identical for either case. This occurs because the first equilibrium [Eq. (2)] is first order both ways and kinetically labile when the reaction in Equation (4) occurs significantly. The cleavage rate constant k_3^{anti} could obviously not be determined since the cleavage does not take place on the time scale of cyclic voltammetry.

In the case of isomer **2** where the intermediate C^- is so frangible that it is never seen in the voltammograms, the only kinetic parameter that can be extracted is the overall rate constant k_{app}^{syn} that includes K_2^{syn} and k_3^{syn}. The parameter $k_{app}^{syn}/k_{1f}^{syn}$ influences the oxidative current of the main wave, as in the previous case, but it influences also the current of the oxidation wave of $[CTC(In)]^-$. The value $k_{app}^{syn} = 20$ s^{-1} gave the best results; it was also necessary to introduce two other homogeneous reactions [Eq. (8) and (9)] involving the products of the cleavage reaction to reproduce simultaneously the size of the oxidation wave of $[CTC(In)]^-$ and the size of the two smaller oxidation waves assigned to [Rh(cod)] residues. These reactions did not affect significantly the parent wave but were required to fit correctly the behaviour of the $[CTC(In)]^-$ wave over time.[14]

$$syn\text{-}[CTC(In)Rh(cod)]^- + [Rh(cod)] \longrightarrow [CTC(In)]^- + [Rh_2(cod)_2] \quad k_4^{syn} \qquad (8)$$

$$[CTC(In)]^- +][Rh(cod)]^+ \longrightarrow \qquad k_5^{syn} \qquad (9)$$

Although not directly apparent from the cyclic voltammograms, a cleavage reaction of the dianion must also be considered [Eq. (10)]. Such a cleavage cannot play a decisive

$$[CTC(In)Rh(cod)]_{B^{2-}} \longrightarrow [CTC(In)]^- + [Rh(cod)]^- \quad k_6 \qquad (10)$$

  0947-6539/99/0511-3361 $ 17.50+.50/0

role, that is it cannot be fast enough to significantly compete with the other reactions, considering that the overall reduction process is reversible at low potential scan rate and a recombination of the would-be anionic fragments appears rather unlikely.

Equation (10) was then introduced into the digital simulation pattern for both isomers and, as expected, the current of the reoxidation peak at -1.4 V in the range of 0.05 to 0.5 V s^{-1} was found to be very sensitive to the value of the corresponding rate constant k_6. The best simulation corresponds to a slow process ($k_6 \leq 0.01\ s^{-1}$), which confirms the higher stability of the dianion compared to the monoanion.

This process, in which one kinetic aspect only is favoured, allowed us to construct a basic set of thermodynamic and kinetic parameters. Variations of each parameter around its initial value were then admissible to reproduce at best the voltammetric behaviour over the whole range of the scan rate. In fact, the values given above are the final values obtained at the start of the process. The fact that no significant variation ($<20\%$) of each parameter was necessary validates a posteriori the procedure used to determine each parameter independently. The remarkable agreement between experimental and predicted voltammograms is illustrated by the set of three voltammograms shown for each isomer in Figure 3 as well as by the agreement between measured individual characteristics and their predicted variations (Figures 2 and 4).

Topological aspects: First of all, the presence of two metals, which coordinate simultaneously to the indenyl ligand, poses the question regarding the first site of reduction. The chromium tricarbonyl group is well known as a strong electron-withdrawing group[15] as well as an electroactive centre; [(arene)$Cr(CO)_3$][16] undergo a bielectronic reduction around -2 V. The compound [(naphtalene)$Cr(CO)_3$], which is isoelectronic with [(indenyl)$Cr(CO)_3$], is reduced at -1.9 V vs. SCE in THF/$n$$Bu_4NBF_4$ with a chemically reversible two electron wave.[17] On the other hand, the rhodium cyclooctadiene group bears a formal positive charge, but the monometallic [(indenyl)Rh(cod)] complex exhibits two reduction waves[2] at more negative potential (-2.42 and -2.7 V) than [(naphtalene)$Cr(CO)_3$]. Bimetallic complexes, **1** and **2**, are reduced at potentials very close to [(naphthalene)$Cr(CO)_3$] and this suggests that the initial electron transfer occurs at the chromium site. However, the cleavage of the radical anions of **1** and **2** to give, on a long time scale, the [(indenyl)$Cr(CO)_3$] anion as discussed above and the absence of any trace of [(indenyl)Rh(cod)] indicate an activation of the rhodium coordination shell.[2]

Thus, it seems likely that the $Cr(CO)_3$ group plays the role of the "antenna", which accepts the first electron and then transfers the "activation" to the rhodium centre. A similar interpretation has been recently made for the oxidation of the bimetallic complex [$Cr(CO)_3$(phenyl)Fc],[18] where a fast internal electron transfer from the oxidised chromium centre to the iron centre has been suggested in the radical cation.

Comparison of the results obtained for the parent monometallic [(indenyl)Rh(cod)] complex (Figure 1c, solid line) shows that the introduction of $Cr(CO)_3$ on the six-membered ring makes the reduction of the complex easier by 560 mV. This is in agreement with its electron-withdrawing properties but it also greatly changes the reactivity associated with the electron transfers and the stability of the generated intermediates. Since the radical anions (form B^-) of the bimetallic complexes are more easily reduced than the corresponding neutral species, we can conclude that the reduction potentials of B^- are at least 830 mV (*anti* isomer) and 900 mV (*syn* isomer) more positive than the values for the radical anion of the monometallic complex.

These data can be more clearly understood if the following points are considered.

1) The presence of the electron-withdrawing group $Cr(CO)_3$ facilitates the initial reduction.
2) The excess electron density in the coordination shell of chromium is reduced by an electronic rearrangement, which involves a change in the hapticity[19] of the bridging indenyl ligand and this in turn leads to a decrease in the coordination number and electronic availability at the rhodium centre. This decrease is responsible for a favourable second reduction (Scheme 2).
3) The dianion, which can be depicted as two 18 electron centres (see below), is thus expected to be quite stable compared with the dianion of the monometallic species, which undergoes a fast cleavage.[2]

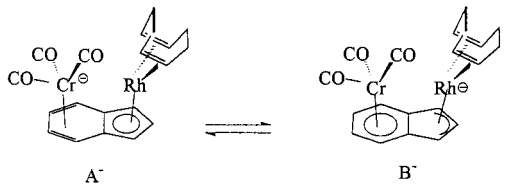

35 [Cr(-I) (17) + Rh(I) (18)] electrons ⇌ *35 [Cr(0) (18) + Rh(0) (17)] electrons*

Scheme 2.

The bimetallic dianions are far more stable than the corresponding monometallic dianion ($k_6 \leq 0.01\ s^{-1}$ against $k^{mono} \geq 1200\ s^{-1}$). The consideration that these formal 36-electron species have a 18+18 close shell configuration should be enough to explain the high stability. Note however that this dianion could not be obtained in preparative electrolysis, since on a long time scale the cleavage of the radical anion, which is formed by conproportionation of the dianion and the neutral parent in solution, prevents the accumulation of the dianion, as shown by the consumption of one Faraday *per* mole and the quantitative formation of the [(indenyl)Cr-$(CO)_3$] anion in the electrolysis.[20]

A comparison between the reduction of *anti* and *syn* isomers indicates that, even if their reduction potentials are almost the same—that is the electronic environments at the metal centres are similar—the peak to peak distance ΔE^p of the reversible reduction wave is greater for the *syn* isomer. It means that the structural rearrangement concomitant with the second electron transfer is more important; the oxidation of the *syn* dianion, which occurs at less negative potential than that of the *anti* isomer, is more difficult and this suggests a

  0947-6539/99/0511-3362 $ 17.50+.50/0 *Chem. Eur. J.* **1999**, *5*, No. 11

greater stabilisation of the added electrons for the *syn* dianion than for the *anti*. A reasonable explanation is that, in the *syn* geometry, the two additional electrons are shared between the two metals placed side by side thus giving rise to a bond interaction, which is not feasible when the metals are on opposite sides as in the *anti* configuration. In the absence of any spectroscopic data,[20] the structure of the dianions remains hypothetical. The electrochemical results described above and their interpretation in terms of a change of hapticity in both coordination shells (isomerisation from A^- to B^-) point to a 17-electron rhodium centre for the monoanion and support the idea of a 18-electron rhodium centre, which bears the two formal charges in the dianion. In the case of the *syn* geometry, the extra stabilisation of the dianion suggests a bonding interaction between the two metals that is better accounted for by a structure with two 17-electron monoanionic centres (18-electron if considering a real bond) and a non-coordinated double bond at the junction of the two rings.

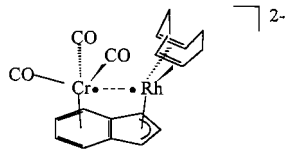

To conclude this section, it must be stressed that these bimetallic compounds do not undergo *trans* to *syn* or *syn* to *trans* interconversion upon electron transfer on the time scale of cyclic voltammetry. This is made clear by repetitive scan voltammetry and by the different patterns observed during the backward oxidation scan of the voltammograms of each isomer.

Conclusion

The two isomers *anti*- and *syn*-[Cr(CO)$_3$(indenyl)Rh(cod)] complexes have 34 electrons shared between the two coordination shells; both metals are coordinatively unsaturated. They are easily reduced at approximately -1.8 V vs. SCE, irrespective of their stereochemistry in an overall reversible bielectronic wave on the time scale of cyclic voltammetry. This situation contrasts with the stepwise reduction (namely two well separated waves vs. a single two-electron wave) of the monometallic [(indenyl)Rh(cod)]. The reason for this different behaviour is to be found in a rearrangement of the monoanion, which makes the second electron transfer easier than the first one. The rearrangement can be depicted as a modification of hapticity of the indenyl ligand. Whatever the *syn* or *anti* structure, the monoanion evolves over a longer time scale and it eventually leads to a decoordination of the rhodium moiety. It has not been possible to characterise all the steps of this decoordination process, which depends on the stereochemistry of the parent complex, yet this probably occurs as suggested before for the monometallic species.[2]

The dianion formed after the two-electron reduction appears to be highly stabilised by the presence of the tricarbonylchromium group. The data obtained here showed that this stabilisation is more pronounced in the *syn* geometry, which supports the hypothesis of a bonding interaction between the two metals in the dianionic form. The existence of such an interaction had already been proposed for the neutral species[21] on the basis of the metal–metal distance and this is reinforced at the two electron reduction stage.

Finally, this electrochemical investigation has shown that the three step general scheme—activation of one metal centre by electron transfer, relaxation by bridging ligand slippage, chemical activation of the second metal—is indeed realistic. The electron demand of the rhodium group, which is observed here by the very easy reduction of the monoanion, is transposable to a coordination unsaturation responsible for enhanced catalytic activity.

Experimental Section

Chemicals and instrumentation: THF (Acros or Carlo Erba) was purified by distillation from Na/benzophenone under an argon atmosphere and then oxygen degassed with vacuum line techniques just before use. Ferrocene (Acros) was purified by recrystallisation before use.

The complexes *anti*-[7b] and *syn*-[Cr(CO)$_3$(indenyl)Rh(cod)][21] were synthesised according to the published procedure. [Cr(CO)$_3$(indenyl)K] salt was prepared at 243 K from a solution of freshly crystallised [Cr(CO)$_3$(indene] and KH (10 equiv) in THF (0.1M) under a blanket of argon, as previously described.[22]

The supporting electrolyte nBu$_4$NBF$_4$ was prepared from nBu$_4$NHSO$_4^-$ and NaBF$_4$, recrystallised from hexane/ethylacetate and dried at 60°C under vacuum.

All the electrochemical experiments were carried out under a blanket of argon. The electrolyses were performed in a two-compartment cell with solutions of the complex (3 mM) in THF (concentration of nBu$_4$NBF$_4$ 0.2M). The working electrode was a 2 cm^2 platinum grid basket, the counter electrode a platinum grid set in the anodic compartment, which had been filled with the same THF supporting electrolyte solution. A Amel Model 731 (integrator) and Model 551 (potentiostat) were used in the electrolyses.

Cyclic voltammetry experiments were performed in an air-tight three-electrode cell, which was connected to a vacuum/argon line. The reference electrode was a SCE (Tacussel ECS C10), which was separated from the solution by a bridge compartment filled with the same solvent/supporting electrolyte solution used in the cell. The counter electrode was a platinum spiral with approximately 1 cm^2 apparent surface area. The working electrodes were disks obtained from the cross section of gold wires of various diameters (0.5, 0.125 mm and 25 μm) sealed in glass. Between each CV scan, the working electrodes were polished on alumina according to standard procedures and sonicated before use.

An EG&G PAR 175 signal generator was used. The potentiostat was home-built with a positive feedback loop for compensation of ohmic drop.[23] The currents and potentials were recorded on Nicolet 310 or Lecroy 9310L oscilloscopes.

Simulations: Digital simulations of the proposed mechanisms were performed with the program Antigona for applied electrochemistry (chronoamperometry and voltammetry) written by Loïc Mottier.[24] It allows the treatment of experimental curves and the comparison with the prediction based on a kinetic mechanism defined by the user. The numerical algorithm is based on the Crank–Nicholson algorithm with a space exponential grid.[25] The program runs under Windows 95 and 3x with the extension Win32 and its running codes can be provided by Dr. Mottier on request.

The voltammograms resulting from the simulation were obtained when using the following set of kinetic data.

***anti* isomer**: reduction of **1**: $E_1^0 = -1.75$ V vs. SCE, $k_1^{0anti} = 2.5 \times 10^{-3}$ cm s^{-1}, $\alpha_1^{anti} = 0.42$; reduction of **1**$^-$: $E_2^0 = -1.62$ V vs. SCE, $k_2^{0anti} = 4 \times 10^{-3}$ cm s^{-1}, $\alpha_2^{anti} = 0.5$; oxidation of C$^-$: $E_3^0 = -0.45$ SCE, $k_3^{0anti} = 4 \times 10^{-3}$ cm s^{-1}, $\alpha_3^{anti} =$

0.5; homogeneous rate constants: $k_{1f}^{anti} = 150\ s^{-1}$, $k_{1b}^{anti} = 150\ s^{-1}$, $k_{2f}^{anti} = 100\ s^{-1}$, $k_{2b}^{anti} = 100\ s^{-1}$ and $k_6^{anti} = 0.01\ s^{-1}$

***syn* isomer**: reduction of **2**: $E_1^0 = -1.71$ V vs. SCE, $k_1^{0syn} = 3.5 \times 10^{-2}\ cm\,s^{-1}$, $\alpha_1^{syn} = 0.55$; reduction of $\mathbf{2}^-$: $E_2^0 = -1.46$ V vs. SCE, $k_2^{0syn} = 4.5 \times 10^{-2}\ cm\,s^{-1}$, $\alpha_2^{syn} = 0.8$; oxidation of $[CTC(In)]^-$: $E_3^0 = -0.30$ V vs. SCE, $k_3^0 = 0.005\ cm\,s^{-1}$, $\alpha_3 = 0.5$; oxidation at -1.6 V assigned to [Rh(cod)]: $E_4^0 = -1.59$ V vs. SCE, $k_4^0 = 0.1\ cm\,s^{-1}$, $\alpha_4 = 0.5$; oxidation wave at -0.8 V: $E_5^0 = -0.87$ V vs. SCE, $k_5^0 = 0.1\ cm\,s^{-1}$, $\alpha_5 = 0.5$; homogeneous rate constants: $k_{1f}^{syn} = 100\ s^{-1}$, $k_{1b}^{syn} = 600\ s^{-1}$, $k_{app}^{syn} = 20\ s^{-1}$, $k_6^{syn} \leq 0.01\ s^{-1}$. The rate constants for the extra homogeneous reactions (8) and (9) were found to be $k_4^{syn} = 4 \times 10^4\ M^{-1}s^{-1}$ and $k_5^{syn} = 10^4\ M^{-1}s^{-1}$.

Determination of the absolute electron stoichiometry:[10] The chrono-amperometric diffusion currents at a 0.5 mm diameter gold electrode for a stepuration of 0.2 s and the steady-state reduction currents at a 12.5 mm radius gold disk microelectrode (potential scan rate $20\ mV\,s^{-1}$) were measured for solutions of **1** and **2** (3 mM) and ferrocene ($D = 8 \times 10^{-6}\ cm^2\,s^{-1}$ under identical conditions (THF 0.28 mol dm^{-3} nBu$_4$NBF$_4$). These data allowed the determination of the absolute consumption of electrons at the reduction wave of **1** and **2** and the diffusion coefficients of these two isomers. For a given period of 0.2 s, the results were as follows for complex **1**. $n_{app} = 2.0 \pm 0.35$, $D = (9.6 \pm 0.1) \times 10^{-6}\ cm^2\,s^{-1}$; for complex **2**: $n_{app} = 1.75 \pm 0.3$, $D = (5.2 \pm 0.5) \times 10^{-6}\ cm^2\,s^{-1}$.

Acknowledgments

This work was supported in part by the University of Padova and CNR for the Italian group and by the Ecole Normale Supérieure, the French Ministry of Education and Research and CNRS for the French group. A bilateral international collaborative research grant from CNR (Italy) and CNRS (France) is also gratefully acknowledged.

[1] a) J. K. Kochi, *Organometallic Mechanism and Catalysis*, Academic Press, New York, **1978**; b) D. Astruc, *Chem. Rev.* **1988**, *88*, 1188; c) D. R. Tyler, *Acc. Chem. Res.* **1991**, *24*, 325; d) N. G. Connelly, W. E. Geiger in *Adv. Organomet. Chem.* **1984**, *23*, 1–93; e) *Organometallic Radical Processes*, (Ed.: W. C. Trogler), J. Organomet. Chem. Library, Elsevier, Amsterdam, **1990**.

[2] C. Amatore, A. Ceccon, S. Santi, J.-N. Verpeaux, *Chem. Eur. J.* **1997**, *3*, 279.

[3] N. G. Connelly, W. E. Geiger in *Adv. Organomet. Chem.* **1985**, *24*, 87–130.

[4] A. L. Lehninger in *Biochemistry*, Worth Publishers, New York, **1970**.

[5] a) M. E. Rerek, L. N. Ji, F. J. Basolo, *J. Chem. Soc. Chem. Commun.* **1983**, 1280; b) J. M. O'Connor, C. P. Casey, *Chem. Rev.* **1987**, *87*, 37; c) A. K. Kakkar, N. J. Tayor, T. B. Marder, J. K. Shen, N. Hallinan, F. Basolo, *Inorg. Chim. Acta* **1992**, *198*, 219; d) G. A. Miller, M. J. Therien, W. C. Trogler, *J. Organomet. Chem.* **1990**, *383*, 271; e) O. V. Gusev, L. I. Denisovich, M. G. Peterleitner, A. Rubezhov, N. A. Ustynyun, P. M. Maitlis, *J. Organomet. Chem.* **1993**, *204*, 15; f) A. Ceccon, C. J. Elsevier, J. M. Ernsting, A. Gambaro, S. Santi, A. Venzo, *Inorg. Chim. Acta* **1993**, *204*, 15.

[6] a) A. Borrini, P. Diversi, G. Ingrosso, A. Lucherini, G. Serra, *J. Mol. Catal.* **1985**, *30*, 181; b) T. B. Marder, D. C. Roe, D. Milstein, *Organometallics* **1988**, *7*, 1451; c) A. Ceccon, A. Gambaro, S. Santi, A. Venzo, *J. Mol. Catal.* **1991**, *69*, L1; J. M. Frankcom, J. C. Green, A. Nagy, A. K. Kakkar, T. B. Marder, *Organometallics* **1993**, *12*, 3688.

[7] a) A. Ceccon, A. Gambaro, S. Santi, A. Venzo, *J. Chem. Soc. Chem Commun.* **1989**, 51; b) C. Bonifaci, G. Carta, A. Ceccon, A. Gambaro, S. Santi, A. Venzo, *Organometallics* **1996**, *15*, 1630.

[8] The X-ray analysis of the ground-state structure for the *syn* and *anti* complexes showed that the *anti* coordination of the benzene ring does not modify the geometry of the rhodium cyclopentadienyl moiety, whilst in the *syn* coordination the structure is strongly modified by the large deviations from planarity of the indenyl frame and the highly distorted coordination of COD to rhodium.[21] Nevertheless the potential reduction of the two isomers is quite similar.

[9] A. J. Bard, L. R. Faulkner, *Electrochemical Methods*, John Wiley, New York, **1980**.

[10] C. Amatore, M. Azzabi, P. Calas, A. Jutand, C. Lefrou, Y. Rollin, *J. Electroanal. Chem.* **1990**, *288*, 45.

[11] The reduction at 0.5 V s^{-1} of $[Rh(cod)(THF)_n]^+$, produced in situ by the addition of $AgPF_6$ (1 equiv) to a solution of dimer $[\{Rh(cod)Cl\}_2]$ (5 mM) in THF, showed two large waves at -1.65 and -2.15 V *vs.* SCE; in a similar way, the reduction of the dimer $[\{Rh(cod)Cl\}_2]$ under the same conditions led to two well defined waves at -1.85 and -2.15 V vs. SCE. The second wave, identical in both voltammograms, must correspond to the reduction of a species formed in both reductive processes, that is the reduction of the $[Rh(cod)(THF)_x]$ radical. Similar intermediates could be produced after the reduction of the *syn* isomer, as suggested in the proposed mechanism. The wave at -1.6 V (Figure 3d) can be assigned to the oxidation of a solvated [Rh(cod)] radical from the results given above (reduction of the corresponding cation) and that at -0.8 V, which appears over a sufficiently long time scale, only can be tentatively assigned to the oxidation of a Rh dimer or cluster $[\{Rh(cod)\}_n]$, which is formed by the association of [Rh(cod)] radicals or reaction of [Rh(cod)] with the *syn* radical anion $[CTC(In)Rh(cod)]_{A/B}^-$.

[12] This relation is easily established from a thermodynamic cycle corresponding to the scheme: $A + e \rightleftharpoons A^-$ (E_1^0); $A^- \rightleftharpoons B^-$ (K_1); $B^- + e \rightleftharpoons B^{2-}$ (E_2^0), by identification of the overall $\Delta G_{app}^0 = -2FE_{app}^0$ with the sum of the three contributions: $-(FE_1^0 + RT\ln K_1 + FE_2^0)$.

[13] The structure of this intermediate C^- cannot be investigated due to its short lifetime; however, since C^- lies part way between [CTC(indenyl)Rh(cod)] and $[CTC(In)]^-$, which is decoordinated from the rhodium centre, a likely structure is the $[CTC(\eta^1\text{-indenyl})Rh]$ complex.

[14] Reaction 9 had to be introduced, in the case of the *syn* isomer, into the simulation pattern to reproduce the size of the waves corresponding to the oxidation of $[CTC(In)]^-$ and [Rh(cod)] residues. This reaction is expected to produce the starting bimetallic complex again by recombination of the fragments and should therefore lead to a scrambling of the stereochemistry. The conversion of a tiny amount of *syn* to *anti* isomer was not detected on the cyclic voltammograms due to the insignificant role of this reaction in the overall scheme.

[15] a) A. Ceccon, *J. Organomet. Chem.* **1974**, *72*, 189; b) A. Ceccon, G. Catelani, *J. Organomet. Chem.* **1974**, *72*, 179.

[16] a) R. D. Rieke, J. S. Arney, W. E. Rich, B. R. Willeford, Jr., B. S. Poliner, *J. Am. Chem. Soc.* **1975**, *97*, 5952; b) A. Ceccon, A. M. Romanin, A. Venzo, *Transition Met. Chem.* **1975**, *1*, 25; c) A. Ceccon, A. M. Romanin, M. Gentiloni, *Gazz. Chim. Ital.* **1976**, *106*, 291; d) A. Ceccon, A. M. Romanin, A. Venzo, *J. Electroanal. Chem.* **1981**, *130*, 245.

[17] R. D. Rieke, W. P. Henry, J. S. Arney, *Inorg. Chem.* **1987**, *26*, 420.

[18] L. K. Jeung, J. E. Kim, Y. K. Chung, P. H. Rieger, D. A. Sweigart, *Organometallics*, **1996**, *15*, 3891.

[19] A similar ring slippage equilibrium has been proposed by some of us for the neutral compound. The proposed equilibrium helps to explain the huge increase in reactivity at both chromium and rhodium centres in stoichiometric and catalytic reactions with respect to the analogous monometallic complexes.[6c, 7b, 18]

[20] Attempts to gain structural IR information and eventually characterise the dianion were not successful as expected. Indeed, in cyclic voltammetry experiments, it is possible to accumulate the dianion in the diffusion layer and reoxidise it back during the reverse scan. Conversely, in any preparative experiment, either chemical or electrochemical, the generated dianion undergoes a fast exergonic conproportionation with the starting complex and forms the monoanion in the bulk solution. In voltammetry, this reaction is partially suppressed because the starting material is almost exhausted in the diffusion layer, whereas it is present in the bulk solution in preparative experiments or in micropreparative experiments such as in a spectroelectrochemical cell. This reaction also explains the bielectronic character of the reduction wave in cyclic voltammetry and the one Faraday consumption in electrolysis. Irrespective of its intrinsic stability, the dianion will thus be consumed at the same rate as the monoanion, which means in the 0.01 to 0.1 s range. There is thus no way to catch the monoanion by spectroelectrochemistry at around room temperature. Electrolyses carried out at $-30\,^\circ C$ gave exactly the same results (one Faraday and cleavage), as well as chemical reductions using one or two molar equivalents of potassium naph-

  0947-6539/99/0511-3364 $ 17.50+.50/0

thalenide at −78 °C. The IR spectrum of the reaction mixture, which was immediately transferred into the IR cell, revealed the spectrum of $[CTC(In)]^-$ only. One referee suggested that a thin-layer optical cell should have been used to perform a spectroelectrochemical investigation under conditions close to those of cyclic voltammetry at low temperature, as previously done by some of us (B. D. Rossenaar, F. Hartl, D. J. Stufkens, C. Amatore, E. Maisonhaute, J.-N. Verpeaux, *Organometallics* **1997**, *16*, 4675.). However, this was not possible here since the OTTLE cell equipment is not available in either of our two groups. In the work cited above, the in situ thin-layer experiments had been performed in Professor F. Hartl's group in Amsterdam as part of a collaboration.

[21] a) C. Bonifaci, A. Ceccon, S. Santi, C. Mealli, R. W. Zoeliner, *Inorg. Chim. Acta*, **1995**, *240*, 541; b) C. Bonifaci, A. Ceccon, A. Gambaro, P. Ganis, S. Santi, G. Valle, A. Venzo, *J. Organomet. Chem.* **1995**, *492*, 35.
[22] A. Ceccon, A. Gambaro, F. Gottardi, S. Santi, A. Venzo, *J. Organomet. Chem.* **1991**, *412*, 85.
[23] C. Amatore, C. Lefrou, F. Pflüger, *J. Electroanal. Chem.* **1989**, *43*, 270.
[24] Present address: Dipartimento di Chimica Fisica
Università degli Studi di Padova
E-mail: mottier@pdchfi.chfi.unipd.it.
[25] B. Speiser in *Electroanalytical Chemistry, a Series of Advances, Vol. 19* (Eds.: A. J. Bard, R. Rubinstein), Marcel Dekker, Basel, **1996**, p. 1.

Received: September 16, 1998 [F1351]